



This is the peer reviewed version of the following article: Allepuz, Alberto, Jordi Casal, and Daniel Beltrán-Alcrudo. 2018. "Spatial Analysis Of Lumpy Skin Disease In Eurasia— Predicting Areas At Risk For Further Spread Within The Region". *Transboundary And Emerging Diseases* 66 (2): 813-822. doi:10.1111/tbed.13090, which has been published in final form at <https://doi.org/10.1111/tbed.13090>. This article may be used for non-commercial purposes in accordance with Wiley Terms and Conditions for Use of Self-Archived Versions <http://www.wileyauthors.com/self-archiving>.

Document downloaded from:





DR. ALBERTO ALLEPUZ (Orcid ID : 0000-0003-3518-1991)

PROF. JORDI CASAL (Orcid ID : 0000-0002-6909-9366)

DR. DANIEL BELTRÁN-ALCRUDO (Orcid ID : 0000-0002-8646-357X)

Article type : Original Article

## **Spatial analysis of lumpy skin disease (LSD) in Eurasia – Predicting areas at risk for further spread within the region**

Alberto Allepuz<sup>\*1,2</sup>, Jordi Casal<sup>1,2</sup>, Daniel Beltrán-Alcrudo<sup>3</sup>

<sup>1</sup>Departament de Sanitat i Anatomia Animals, Facultat de Veterinària, UAB, 08193 Bellaterra, Barcelona, Spain.

<sup>2</sup>Centre de Recerca en Sanitat Animal (CReSA, IRTA-UAB), Campus de la Universitat Autònoma de Barcelona, 08193 Bellaterra, Spain.

<sup>3</sup>Food and Agriculture Organization (FAO), Regional Office for Europe and Central Asia, Budapest, Hungary

\*Corresponding Author: [alberto.allepuz@uab.cat](mailto:alberto.allepuz@uab.cat)

### **Abstract**

Data from affected lumpy skin disease (LSD) locations between July 2012 and September 2018 in the Balkans, Caucasus and Middle East were retrieved from FAO's Global Animal Disease Information System (EMPRES-i) from the European Commission's Animal Disease Notification System (ADNS) and completed with data from the official veterinary services of some countries. During this period, a total of 7,593 locations from twenty-two countries were affected. Within this period, over 46,000 cattle were clinically affected by LSD, 3,700 animals died and 17,500 were slaughtered due to culling policies to stop the spread of the disease. Most outbreaks occurred in 2016, between the months of May and November.

This article has been accepted for publication and undergone full peer review but has not been through the copyediting, typesetting, pagination and proofreading process, which may lead to differences between this version and the Version of Record. Please cite this article as doi: 10.1111/tbed.13090

This article is protected by copyright. All rights reserved.

The affected region was divided in a grid of 10 x 10 km cells and we fit a spatial regression model to analyse the association between the reported LSD outbreaks and climatic variables, land cover and cattle density. The results showed big differences in the odds of being LSD positive due to the type of land cover: the odds of a cell being LSD positive was increased in areas mostly covered with croplands, grassland or shrubland. The odds was also increased for higher cattle density, as well as areas with higher annual mean temperature and higher temperature diurnal range. The resulting model was utilized to predict the LSD risk in neighboring unaffected areas in Europe, the Caucasus and Central Asia, identifying several areas with high risk of spread. Results from this study provide useful information for the design of surveillance and awareness systems, and preventive measures, e.g. vaccination programs.

**Key words: Lumpy Skin Disease, Spatial Analysis, Risk Assessment**

### **Introduction**

Lumpy skin disease (LSD) is an emerging viral disease of cattle and Asian water buffalo that can have an important impact in livestock production and trade. The disease, characterised by the appearance of nodules on the skin and in the respiratory, digestive and genital tracts, is caused by a *Capripoxvirus* of the *Poxviridae* family (Tuppurainen and Oura, 2012). The disease was initially restricted to Sub-Saharan Africa, but in the eighties of the last century, the disease spread to Egypt and the Middle East. In 2012 the disease appeared again in the Middle East, spread into Turkey, and from there west into the Balkans, and east into the Caucasus, the south of the Russian Federation and Kazakhstan, generating great concern (Tuppurainen et al., 2017).

The mechanisms by which lumpy skin disease virus (LSDV) is transmitted between animals is not completely clear. The main transmission mechanism has been suggested to be a variety of blood-feeding vectors that would mechanically transmit the virus between animals (EFSA, 2015). However there is very little information on the arthropod actually involved in spreading the disease, especially in the newly affected regions. Despite the absence of strict evidence, Diptera insects and Ixodid ticks have been associated with LSD transmission. *Stomoxys calcitrans*, a cosmopolitan species of Muscidae, has been associated with the introduction and spread of LSD in Israel (Kahana-Sutin et al., 2017). *Haematobia irritans*, another species of Muscidae, has been also implicated in the transmission of LSD in beef herds in Israel, but without formal evidence (Kahana-Sutin et al. 2017). Within the Culicidae, Chihota et al. (2001) demonstrated the transmission by *Aedes aegypti* from viraemic cattle to recipient animals under experimental conditions. The role of ticks, probably as mechanical vectors, has been demonstrated experimentally for three species from sub-Saharan Africa (Lubinga et al., 2014), but there is no data about the possible role of the species present in the new affected areas.

Transmission through semen has been suggested as LSDV was isolated from semen (Irons et al., 2005) from the testis and epididymis of infected bulls (Annandale et al., 2010) and heifers were infected after being inseminated with LSDV experimentally infected semen (Annandale et al., 2014). Vertical transmission (Rouby et al., 2016) iatrogenic transmission due to the use of contaminated needles in different animals and transmission to suckling calves through skin lesions in the teat (Tuppurainen et al., 2017) have also been suggested to play a role in the spread of the virus. Nevertheless, it is generally assumed that LSDV is transmitted inefficiently by direct contact between infected and susceptible animals (Carn et al., 1995; EFSA, 2015).

Due to the fact that vectors play a key role in LSDV transmission, the spread and geographical distribution of the disease is likely to be heavily influenced by climatic conditions, and the presence of surface water, where vectors are more prevalent. However, there have been few attempts to model the spatial distribution of LSD (Alkhamis and VanderWaal, 2016).

Therefore, the objective of this study was to analyse and identify the association between the reported LSD outbreaks (in Turkey, the Russian Federation, the Balkans and Israel) with climatic variables, land cover and cattle density in order to predict the risk of LSD spread in neighboring unaffected countries of Europe and Central Asia. The results of this study provide useful information for the design of surveillance and awareness systems, and preventive measures, e.g. vaccination programs.

## **Materials and methods**

### **Data:**

The basic data related to the different LSD affected locations (e.g. date, geographical coordinates and at risk, affected and dead animals) between July 2012 and December 2018 in the Balkans, Caucasus and Middle East were extracted from the Global Animal Disease Information System (EMPRES-i) of the Food and Agriculture Organization of the United Nations (FAO) and from the European Commission's Animal Disease Notification System (ADNS). More detailed information, e.g. the number of affected locations, was obtained directly from the official sources of Albania, Kosovo, the Former Yugoslav Republic of Macedonia, Montenegro and the Russian Federation. Geographical coordinates from Montenegro, Kosovo and the Former Yugoslav Republic of Macedonia were not provided so the location where the animals were registered was used. Coordinates of the affected villages were extracted from Google Map Developers web page (<http://www.mapdevelopers.com/index.php>), BingMaps (<https://www.bing.com/maps>), GoogleMaps (<https://www.google.com/maps>) and Mapquest (<https://developer.mapquest.com>). The date of the first case reported at each location minus a 28-day incubation period, as described in the OIE Terrestrial Manual was considered as the date of infection.

For the spatial analysis, we selected the following variables:

- Density of cattle: obtained from FAO (Nicolas et al., 2016) at a 5km<sup>2</sup> resolution, with the source cattle data actually dating from 2010.
- Land cover: we used the 0.5 km MODIS-based Global Land Cover, available from the United States Geographical Survey (USGS) webpage that classifies land cover in 16 different features including water bodies, different types of forest, shrublands and savannas, croplands, urban areas and sparsely vegetated areas (Broxton et al., 2014). For the analysis we grouped the 16 categories into seven: i) Water, urban and snow and ice categories (where no susceptible host species are expected to be present); ii) Forest (including all forest categories); iii) Shrublands and savannas; iv) Grasslands; v) Permanent wetlands; vi) Cropland and natural vegetation mosaic; and vii) Barren or sparsely vegetated areas.
- Climate raster data: we obtained the 19 bioclimate variables available at the worldclim webpage at a 5km<sup>2</sup> resolution. These included the annual mean temperature, temperature and precipitation ranges, etc., average values for the years 1970 to 2000 (Fick et al., 2017).

For modelling purposes, we divided the area of study into a regular grid of 10km by 10km cells. In order to evaluate risk factors for LSD spread while minimizing the effect of vaccination as a confounder, we considered a mask composed only by grid cells from geographical areas where disease spread was not influenced by vaccination or such influence was assumed to be minimal. This was done by i) choosing only the areas within each country where the disease had already spread by the time vaccination started (i.e. Israel, the south of Serbia, Kosovo, the south of Bulgaria, Former Yugoslav Republic of Macedonia, Albania, Montenegro and the border of Greece with Turkey). When choosing the cutoff vaccination date, we considered that it would take 3 weeks for cattle to develop immunity; and ii) assuming that even when vaccination was applied, it was not very effective to halt the spread of the disease. This would be the case of Turkey and the affected parts of the Russian Federation. These two countries used attenuated sheep pox vaccines, which have been proven to be inferior to the Neethling attenuated vaccines successfully utilized in the Balkans (Ben Gera et al., 2015). In addition, in Turkey, LSD was reported for the first time in mid-2013 in the southern provinces. By 2014, LSD had arrived to areas 500 km away from the initial cases (Sevik and Dogan, 2016) and the vaccination coverage was considered to be too low to halt the spread of the disease (EFSA, 2015). In the Russian Federation, the first outbreaks occurred close to the border with Georgia and Azerbaijan in July 2015 and, as in Turkey, by 2016 LSD had spread a long distance from the first outbreaks (Sprygin et al., 2018). The lack of a vaccine efficiency control was blamed as one of the causes for this uncontrolled spread (EFSA, 2017). Outbreaks in the Middle East and the Caucasus, despite being affected, were not considered due to the very few positive cells, believed to be due to a high degree of under-reporting. The LSD status of a grid cell was considered as positive if it contained at least one positive location and negative otherwise. We used the assumption that, even with some degree of under-reporting, a 10km grid cell would account for areas where LSD outbreaks may be present.

Neighborhood countries still not affected by LSD and those parts of countries not included in the analysis were also divided in 10km grid cells to perform model predictions. This was the case of parts of Southeast Europe (Bosnia, Cyprus, Romania, plus parts of Bulgaria, Greece and Serbia), Eastern Europe (Belarus, Moldova and Ukraine), Near East (Jordan, Lebanon and Syria), the Caucasus (Armenia, Azerbaijan and Georgia) and Central Asia (Kazakhstan, Kyrgyzstan, Tajikistan, Turkmenistan and Uzbekistan).

The cattle density raster was superimposed on this 10km grid cell, and those cells with zero cattle density were removed from the analysis. Figure 1 represents the areas included in the analysis either for model calibration or for performing predictions. Finally, each of the 21 raster layers with the covariates data were superimposed on this grid in order to extract the data for further analysis. All of these analyses were performed with Quantum GIS (QGIS Development Team, 2017).

### Statistical analysis:

The 70% of grid cells of the mask used for model calibration were randomly selected. In this dataset, the pairwise Spearman's correlation coefficient between each variable (with the exception of land cover, which is not a continuous variable), was calculated using the 'cor' function in the contributed package corrplot (Taiyun et al., 2017). Only those variables with a correlation coefficient lower than the absolute value of 0.7 were considered for the multivariable model. The probability of a grid cell being LSD-positive each year ( $p_i$ ) was modelled by assuming a Bernoulli distribution for the status of each of the grid cells. Therefore, to link the probability of infection of each grid cell with specific explanatory variables, we used the logit transformation.

A backward and forward stepwise procedure based on the Akaike Information Criterion (AIC) was used to select the best model. To test for spatial autocorrelation in model residuals, we plotted as a correlogram the Moran's I statistic from the 1<sup>st</sup> to the 8<sup>th</sup> spatial neighborhood using the spdep package (Bivand et al., 2015; Bivand et al., 2013). The Moran's I statistic quantifies the similarity of a value between areas defined as neighbors (i.e. if they share a single boundary point) (Moran, 1950). The Moran's I statistic value ranges from -1 to +1, and when no correlation exists between neighboring areas, the value approximates to zero (Pfeiffer et al., 2008). Due to evidence of spatial autocorrelation in the model residuals, we extended the model by adding spatially structured and unstructured components as follows:

$$\text{logit}(p_i) = ZX + U_i + S_i$$

Where ' $p_i$ ' represent the probability of a grid cell being LSD infected, ' $ZX$ ' the different fixed effects (i.e. density of cattle, climate variables, etc.) and ' $U_i$ ' and ' $S_i$ ' represent the spatially structured and unstructured random effects, respectively. The spatially structured random effect was defined by a stochastic partial differential (SPDE) (Lindgren et al., 2011) and calculated from a matrix of Euclidean distances between centroids of each grid cell using Delaunay triangulation (Simpson et al., 2011; Cameletti et al., 2012). This model was solved by using the R-INLA package (Schrödle and Held, 2011) and we tested again model residuals

to check the presence of spatial autocorrelation by using the same procedure previously explained.

To assess the association of the variables included in the model with random effects with the probability of a grid cell being LSD infected; 95% credible intervals (CR) were obtained from the exponential of the mean, 2.5% and 97.5% percentiles of the posterior probability distribution of the regression coefficients. We considered a variable to be associated if the probability was over 95%, i.e. if the 95% CR was greater or lower than 1. If greater, the variable increased the risk of LSD infection, and if lower, it decreased the risk.

The 30% of grid cells not used for the previous model were used for model validation and a receiver operating characteristic (ROC) curve was constructed to test the ability of the model to discriminate between positive and negative grid cells using the pROC package (Robin et al., 2011) in R. The area under the curve (AUC) is related to the performance of the model. AUC values greater than 0.8 and between 0.7 and 0.8 were indicative of good and moderate discriminate capacities, respectively. Model predictions were made in non-affected areas by using the same model.

## Results

### Descriptive results

A total of 7,593 locations from twenty-two different countries were affected between July 2012 and December 2018 in the region, with most of outbreaks occurring in 2016 and between the months of May and November (figures 2 and 3). Within the whole period, more than 46,000 animals were clinically affected by LSD, around 3,700 animals died and 17,500 were slaughtered due to culling policies to stop the spread of the disease (table 1). Figure 4 shows the reported morbidity and mortality, which was calculated for 5,857 and 5,835 locations, respectively, as the number of affected or dead animals was not always available. The observed morbidity and mortality in each location was very variable (range of 0 to 100%) with a median value of 1.4% and 0% respectively (i.e. in most of locations, no mortality was observed). It has to be taken into account that in some locations the number of animals was very low, as evidenced in the plot of figure 4, where the median is around 90 animals, but the range goes from 1 to 7,500.

### Spatial analysis

The pairwise Spearman correlation matrix showed a high correlation between several environmental variables. Predictors considered for the multivariable model where the annual mean temperature (°C), the mean diurnal temperature range (i.e. the mean of the monthly maximum temperature (°C) minus the monthly minimum temperature (°C)), the temperature seasonality (i.e. the standard deviation \*100), the mean temperature (°C) of the wettest quarter, the annual precipitation (mm) and the seasonality in precipitation (i.e.

the coefficient of variation). Cattle density (cattle per km<sup>2</sup>) and land cover were also considered for the multivariable model. Based on the AIC value, the best fit model included all the above variables. However, the correlogram evidenced that there was some residual spatial autocorrelation. This issue was solved by the inclusion of spatial random effects in the model as can be observed in figure 5 where the Moran's I statistic (and its 95% confidence interval) for both models residuals at 1–8 spatial neighborhoods are shown.

The area under the ROC curve generated using predictions in the 30% of grid cells reserved for model validation was 0.81 indicative of a model with good ability to discriminate between LSD positive and negative grid cells (figure 6).

Odds ratio and their 95% credible intervals (CI) for each of the risk factors from the hierarchical Bayesian model together with the random effects are represented in table 2. The spatial structured random effect had a high variance and accounted therefore for most of the variance explained by the random effects (i.e. 96%). An important finding was the big differences in the odds of being LSD positive due to the type of land cover, i.e. areas with sparse vegetation had a lower risk of infection compared to those mostly covered by forest. On the other hand, areas dominated by croplands, grassland or shrublands showed a higher risk than forested areas. The odds of a grid cell being LSD positive was increased also by the density of cattle, as well as two climatic variables: the annual mean temperature and the mean temperature diurnal range.

The predicted probabilities of LSD spread in the region are shown in figure 7. Some areas show a higher risk of spread. In Central Asia, the highest probability of LSD spread was predicted in the southern part. That is also the case of Ukraine and Romania. In Syria, high risk areas are mostly in the west and northern parts, while in Jordan they are mainly located in the north-west and eastern parts of the country. In the Caucasus, the lowlands show the highest risk.

## Discussion

In this study, we investigated the role of climatic variables, land cover and cattle density in the spatial distribution of LSD outbreaks in an extensive area without taking into account country boundaries. This approach is reasonable as LSD is believed to be transmitted mainly by blood-feeding arthropods and, therefore, political barriers such as country boundaries, are not efficient to stop the spread of the disease. Nevertheless, some long distance jumps have occurred due to human-mediated transportation of cattle between farms, regions or countries, and even by wind transmission (Klausner et al 2018; Mercier et al. 2018).

The results of our model point out the importance of the temperature and the temperature range as predictors of LSD outbreaks, with higher values increasing the risk of LSD outbreaks. The temperature range reflects the fluctuations in temperature along the year, being large values an indicator of greater variability of temperature (O'Donnell et al., 2012).



Results are quite similar to the model developed by Alkhamis and Vander Waal (2016), which focused in the Middle East between 2012 and 2015, despite different approaches to relate climate variables were used. Their ecological niche model identified annual precipitation, land cover and a variable related with temperature (i.e. mean diurnal range) as important predictors for LSD outbreaks. Also, in southern Africa, Tuppurainen et al. (2012) associated LSD outbreaks with wet and warm conditions. In Ethiopia, Gari et al. (2010) and Molla et al. (2017) observed a higher prevalence of LSD in warm and humid agro-climates. This likely reflects the weather conditions needed for vector survival.

In our analysis, the odds of an LSD outbreak in grid cells predominantly covered by croplands was 2.1 (95% CR: 1.2 to 2.5) times the odds of an LSD outbreak in forested areas (table 2). The presence of favorable conditions for vector survival could be an important explanation for the observed differences in the risk of infection due to the land cover type, but there could be several more. For example, proximity to urban areas could facilitate surveillance, thus increasing the number of detected outbreaks. This has been observed elsewhere in the context of foot and mouth disease (Hamoonga et al., 2014; Allepuz et al., 2015). Also, certain land cover types may be more suitable for cattle grazing, thus enabling the mixing of animals of different origins and, therefore, enhancing the transmission of the disease. Indeed, communal grazing and watering points have been reported as risk factors for LSD transmission (Gari et al., 2010).

Another important factor influencing the spatial spread of the disease is the implementation of vaccination programs. In 2016, mass vaccination of cattle was implemented in all affected countries in the Balkans, Turkey, the Russian Federation and the Caucasus. Thanks to the intensive vaccination campaigns, the western spread of the disease is believed to have been controlled (EFSA, 2018). To avoid any confusion due to vaccination, we calibrated the model with data from areas where LSD has spread mainly randomly.

The data used for this study were based on mostly passive reports by the veterinary services from the different countries. The use of passive surveillance data has some limitations that should be considered when interpreting the results. That is especially important in some countries where, for conflict reasons, surveillance would be difficult to implement. Similarly, the presence/quality of compensation programs, the capacity and transparency of veterinary services, the remoteness of some areas, the level of awareness among farmers, etc., in some countries will also hinder reporting. However, in spite of the inevitable limitations in data of this type, we were able to identify biologically plausible risk factors for LSD. We believe that aggregating the data to 10 x 10 km grids and expressing the outcome of interest as a dichotomous variable (i.e. LSD positive, LSD negative), as opposed to a count of the number of outbreaks per grid, minimized the impact of the bias created by the varying intensity of reporting that would be typically present in the study data set.

Our risk map (Figure 7) identifies the areas where LSD could have a higher probability of spread if it arrived. When looking at the latest reported outbreaks, one can make some predictions on its potential spread. The disease seems to be under control in the Balkans,

with no outbreaks reported in 2018 after the massive vaccination (EFSA, 2018), thus limiting the risk of further spread to Central and Southeastern Europe. However, outbreaks continue to be reported from Turkey, Georgia and the Russian Federation. From Turkey, LSD could spread to Syria and Iraq, where the current situation of armed conflict and instability would most likely prevent an effective control of the disease. This is, if the disease is not already circulating unreported. The isolated outbreak in Georgia implies that the virus is probably circulating and the risk of further spread in the Caucasus probably still remains.

Within the Russian Federation, the epidemic seems most active in its eastern front, with numerous outbreaks reported in 2017-2018 along the border with Kazakhstan, mostly in backyard holdings. This constitutes a very real threat of further spread into Central Asia and beyond, where the disease has never been reported before and where cattle is the most important livestock species together with sheep. Over 24 million heads of cattle, plus 25,000 buffaloes (as per FAOSTAT data of 2016) are under risk of LSD in Central Asia. On the other hand, LSD spread westwards within the Russian Federation has come to a halt during 2018, thus reducing the risk of further spread to Ukraine or Belarus. Nevertheless, the possibility of long jumps due to the movement of infected cattle remains, meaning that also countries far away from the active epidemic foci are also at risk.

In conclusion, the risk of LSD infection was linked to cattle density, the type of land cover and climate variables related with temperature. These results enabled the development of a risk map in still unaffected areas in some countries of Europe, the Caucasus and Central Asia. This information could be useful for veterinary services for the development of risk based surveillance, vaccination and general awareness programs by targeting cattle in high risk areas.

### **Acknowledgements**

The authors would like to acknowledge the outbreak data providers for the following national agencies: the Sector of Epidemiology and Identification Registration at the Ministry of Agriculture and Rural Development (Albania), the Food and Veterinary Agency (Kosovo), the Food and Veterinary Agency (the Former Yugoslav Republic of Macedonia), the Food Safety, Veterinary and Phytosanitary Affairs Agency (Montenegro), and the Federal Research Center for Virology and Microbiology (VNIIVVIM; Russian Federation). Acknowledgements also go to the Food and Agriculture Organization of the United Nations (FAO), which financed the study through a Technical Cooperation Project facility (TCPf) titled TCP/RER/643351: Improving the understanding, awareness, prevention and control of lumpy skin disease in the Balkans. The views expressed in this information product are those of the authors and do not necessarily reflect the views or policies of FAO.

## References

Alkhamis, M.A. and K. Vander Waal. (2016). Spatial and Temporal Epidemiology of Lumpy Skin Disease in the Middle East, 2012–2015. *Frontiers in Veterinary Science*. 3, 19

Allepuz, A., M. Stevenson, F. Kivaria, D. Berkvens, J. Casal and A. Picado. (2015). Risk factors for foot-and-mouth disease in Tanzania, 2001-2006. *Transboundary and Emerging Diseases*. 62, 127-36.

Annandale, C.H., Irons, P.C., Bagla, V.P., Osuagwuh, U.I., Venter, E.H. (2010). Sites of persistence of lumpy skin disease virus in the genital tract of experimentally infected bulls. *Reproduction in Domestic Animals*. 45, 250–255.

Annandale, C.H., Holm, D.E., Ebersohn, K., Venter, E.H. (2014). Seminal transmission of lumpy skin disease virus in heifers. *Transboundary and Emerging Diseases*. 61,443–448.

Ben-Gera, J., Klement, E., Khinich, E., Stram, Y., Shpigel, N.Y. (2015). Comparison of the efficacy of Neethling lumpy skin disease virus and x10RM65 sheep-pox live attenuated vaccines for the prevention of lumpy skin disease - The results of a randomized controlled field study. *Vaccine*. 38, 4837-4842.

Bivand, R. and G. Piras. (2015). Comparing Implementations of Estimation Methods for Spatial Econometrics. *Journal of Statistical Software*. 63, 1-36.

Bivand, R. S., J. Hauke and T. Kossowski. (2013). Computing the Jacobian in Gaussian spatial autoregressive models: An illustrated comparison of available methods. *Geographical Analysis*. 45, 150-179.

Broxton, P.D., X. Zeng, D. Sulla-Menashe, P.A., Troch. (2014). A Global Land Cover Climatology Using MODIS Data. *Journal of Applied Meteorology and Climatology*. 53, 1593-1605.

Cameletti, M., Lindgren, F., Simpson, D., Ruem H. (2013). Spatio-temporal modeling of particulate matter concentration through the SPDE approach. *Advances in Statistical Analysis*. 97, 109-131.

Carn, V.M., Kitching, R.P. (1995). An investigation of possible routes of transmission of lumpy skin disease virus (Neethling). *Epidemiology and Infection*. 114, 219-226.

Chihota, C.M., Rennie, L.F., Kitching, R.P., Mellor, P.S. (2001). Mechanical transmission of lumpy skin disease virus by *Aedes aegypti* (Diptera: Culicidae). *Epidemiology and Infection*. 126, 317-321.

EFSA AHAW Panel (EFSA Panel on Animal Health and Welfare). (2015). Scientific Opinion on lumpy skin disease. *EFSA Journal*. 13.

EFSA (European Food Safety Authority). (2017). Scientific report on lumpy skin disease: I. Data collection and analysis. *EFSA Journal*. 15.

EFSA (European Food Safety Authority). (2018). Scientific report on lumpy skin disease II. Data collection and analysis. *EFSA Journal* 2018. 16.

Fick, S.E. and R.J. Hijmans. (2017). Worldclim 2: New 1-km spatial resolution climate surfaces for global land areas. *International Journal of Climatology*.

Gari, G., A. Waret-Szkuta, V. Grosbois, P. Jacquiet, and F. Roger. (2010). Risk factors associated with observed clinical lumpy skin disease in Ethiopia. *Epidemiology and Infection*. 138, 1657–1666.

Hamoonga, R., M.A. Stevenson, A. Allepuz, T.E. Carpenter and Y. Sinkala. (2014). Risk factors for foot-and-mouth disease in Zambia, 1981-2012. *Preventive Veterinary Medicine*. 1, 64-71.

Irons, P.C., Tuppurainen, E.S., Venter, E.H. (2005). Excretion of lumpy skin disease virus in bull semen. *Theriogenology*. 63, 1290–1297.

Kahana-Sutin, E., E. Klement, I. Lensky and Y. Gottlieb (2017). High relative abundance of the stable fly *Stomoxys calcitrans* is associated with lumpy skin disease outbreaks in Israeli dairy farms. *Medical and Veterinary Entomology*. 31, 150-160.

Klausner, Z., Klement, E., Fattal, E. (2017). Source-receptor probability of atmospheric long-distance dispersal of viruses to Israel from the eastern Mediterranean area. *Transboundary and Emerging Diseases*. 65, 205-212.

Lindgren, F., Rue, H., Lindstrom, J. (2011). An explicit link between Gaussian fields and Gaussian Markov random fields: the SPDE approach (with discussion). *Journal of the Royal Statistical Society. Series B*, 73,423–98.

Lubinga, J. C., E. S. M. Tuppurainen, J. A. W. Coetzer, W. H. Stoltsz, and E. H. Venter. (2014). Transovarial passage and transmission of LSDV by *Amblyomma hebraeum*, *Rhipicephalus appendiculatus* and *Rhipicephalus decoloratus*. *Experimental and Applied Acarology*. 62, 67-75.

Mercier, A., Arsevska, E., Bournez, L., Bronner, A., Calavas, D., Cauchard, J., Falala, S., Caufour, P., Tisseuil, C., Lefrançois, T., Lancelot, R. (2018). Spread rate of lumpy skin disease in the Balkans, 2015-2016. *Transboundary and Emerging Diseases*. 65, 240-243.

Molla, W., M.C.M. de Jong and K. Frankena. (2017). Temporal and spatial distribution of lumpy skin disease outbreaks in Ethiopia in the period 2000 to 2015. *BMC Veterinary Research*. 6, 310.

Moran, P. A. P. (1950). Notes on continuous stochastic phenomena. *Biometrika* 37, 17–23.

Nicolas, G., T,P, Robinson., G.R.W. Wint, G. Conchedda, G. Cinardi, M. Gilbert. (2016) Using random forest to improve the downscaling of global livestock census data. *Plos ONE* 11, 3.

O'Donnell, M.S., and D.A. Ignizio. (2012). Bioclimatic predictors for supporting ecological applications in the conterminous United States: U.S. Geological Survey Data Series. 691.

Pfeiffer, D., T. Robinson, M. Stevenson, K. Stevens, D. Rogers, and A. Clements (2008). *Spatial Analysis in Epidemiology*. Oxford University Press, New York.

QGIS Development Team, 2017: QGIS Geographic Information System. Open Source Geospatial Foundation Project. Retrieved from <http://qgis.osgeo.org>.

Robin, X., N. Turck, N. Tiberti, F. Lisacek, J. C. Sanchez, and M. Müller (2011). pROC: an open-source package for R and S+ to analyze and compare ROC curves. *BMC Bioinformatics* 12, 77.

Rouby, S. and E. Aboulsoud (2016). Evidence of intrauterine transmission of lumpy skin disease virus. *The Veterinary Journal*. 209, 193-195.

Schrödle, B. and L. Held (2011). Spatio-temporal disease mapping using INLA. *Environmetrics*. 22, 725–34.

Şevik, M., Doğan, M. (2016). Epidemiological and Molecular Studies on Lumpy Skin Disease Outbreaks in Turkey during 2014-2015. *Transboundary and Emerging Diseases*. 64, 1268-1279.

Simpson, D., Illian, J., Lindgren, F., Sørbye, S.H., Rue, H. (2011). Going off grid: Computationally efficient inference for log-Gaussian Cox processes. NTNU Technical report, 10.

Sprygin, A., Artyuchova, E., Babin, Y., Prutnikov, P., Kostrova, E., Byadovskaya, O., Kononov, A. (2018). Epidemiological characterization of lumpy skin disease outbreaks in Russia in 2016. *Transboundary and Emerging Diseases*. [Epub ahead of print]

Taiyun, W. and S. Viliam. (2017). R package "corrplot": Visualization of a Correlation Matrix (Version 0.84). Retrieved from <https://github.com/taiyun/corrplot>

Tuppurainen E. S. and C.A. Oura. (2012). Review: lumpy skin disease: an emerging threat to Europe, the Middle East and Asia. *Transboundary and Emerging Diseases*. 59, 40–48.

Tuppurainen, E., T. Alexandrov and D. Beltrán-Alcrudo. (2017). Lumpy skin disease field manual –A manual for veterinarians. FAO Animal Production and Health Manual No. 20. Rome. Food and Agriculture Organization of the United Nations (FAO).

Table 1. Descriptive analysis of lumpy skin disease outbreaks by country (2012-2018)

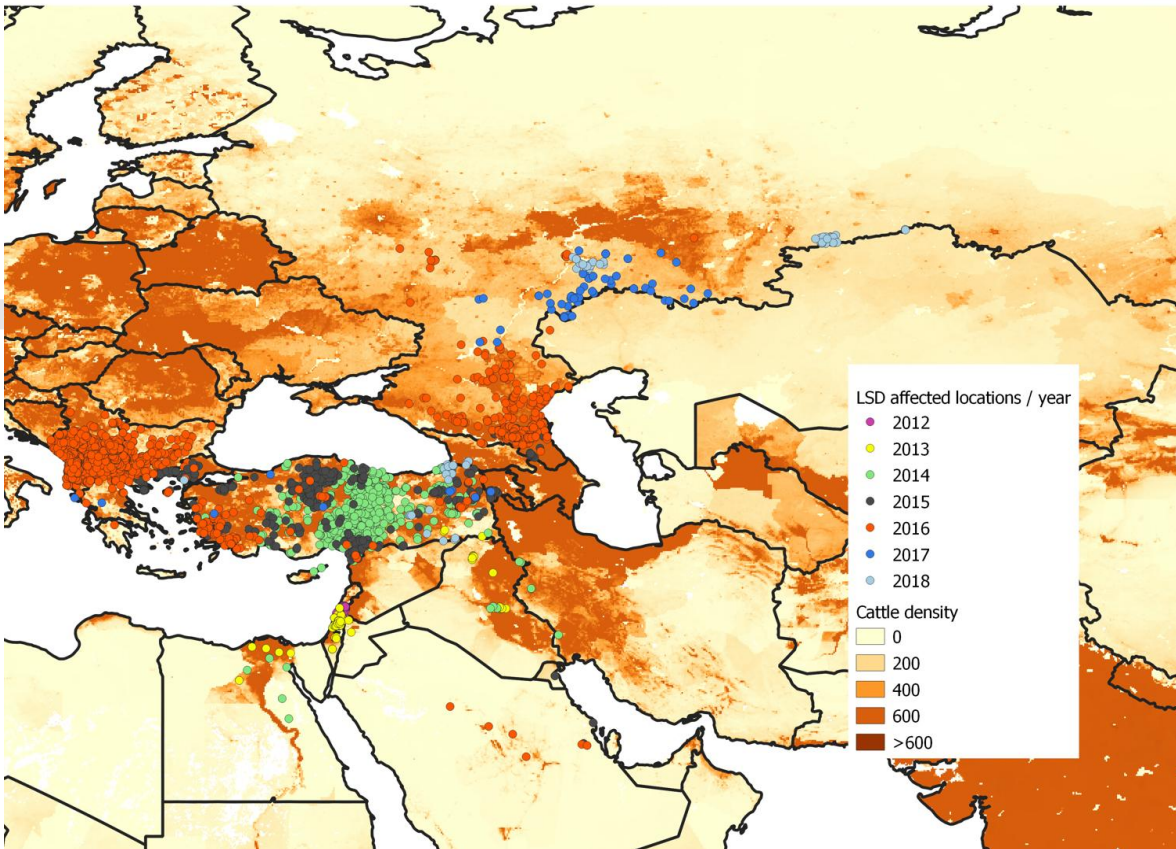
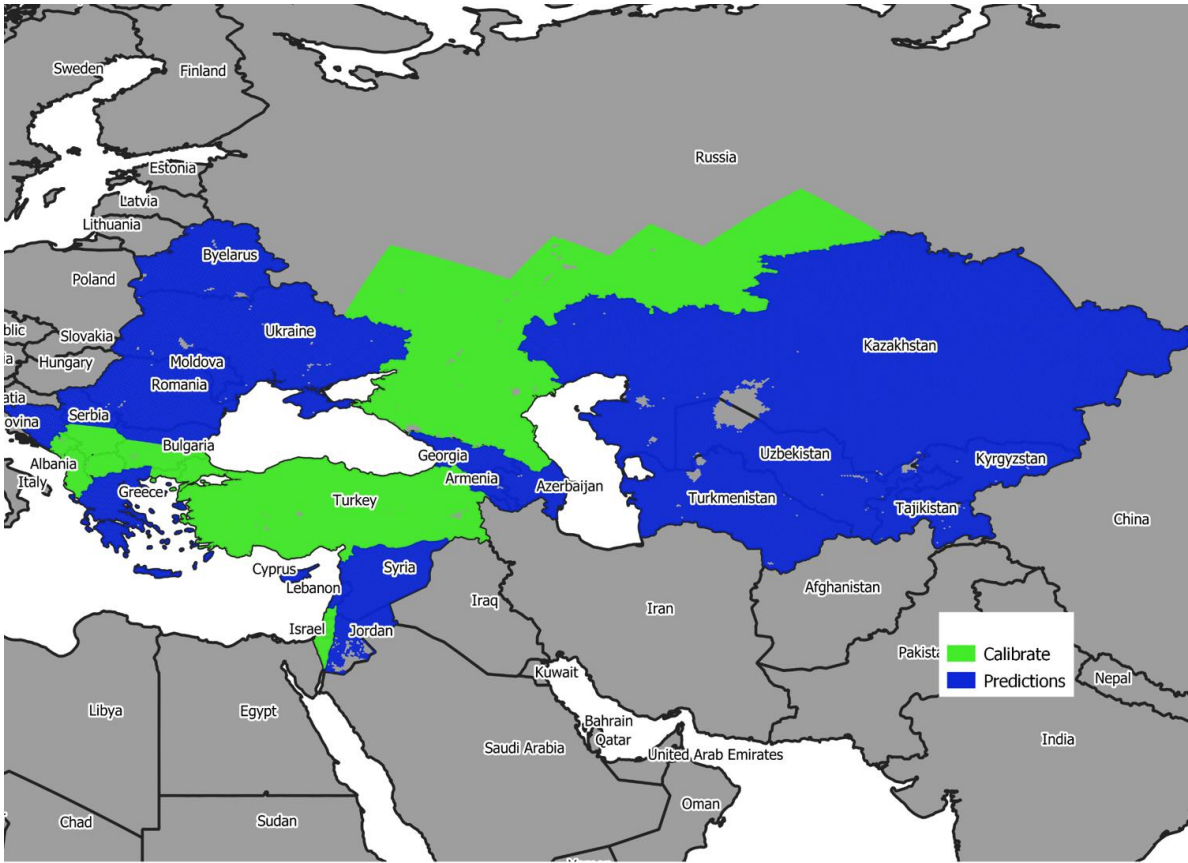
Country	Nr affected locations	Nr of affected animals	Nr of death animals	Nr of slaughtered animals
Albania	3568	4854	1659	
Bulgaria	217	333	24	2190
Cyprus	2			
Egypt	12	6	0	0
Former Yugoslav Republic of Macedonia	472	1064	339	
Georgia	7	11	0	0
Greece	223	817	96	7794
Iran	5	19	0	
Iraq	28	73	7	
Israel	213	3125	74	0
Jordan	2	12	12	0
Kazakhstan	2	460	34	0
Kosovo†	466	2001		
Kuwait	5	196	7	
Lebanon	34	104	4	0
Montenegro	154	271	0	181
Russian Federation	453	15915	2	10
Saudi Arabia	10	11808	455	2201
Serbia	225	357	9	1159
TURKEY	1446	4815	981	3928
West Bank	49	208	59	0
<b>Total</b>	7593	46449	3762	17463

† This designation is without prejudice to positions on status and is in line with United Nations Security Council Resolution 1244 and the International Court of Justice opinion on the Kosovo Declaration of Independence.

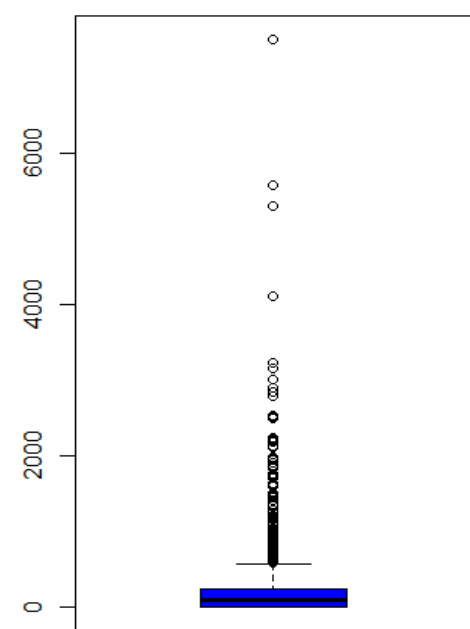
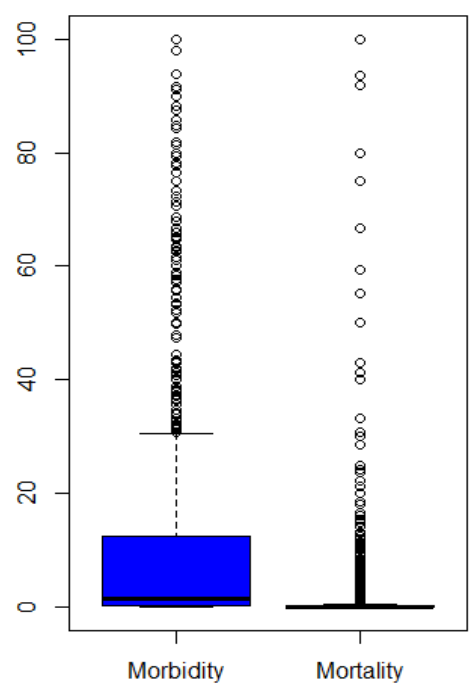
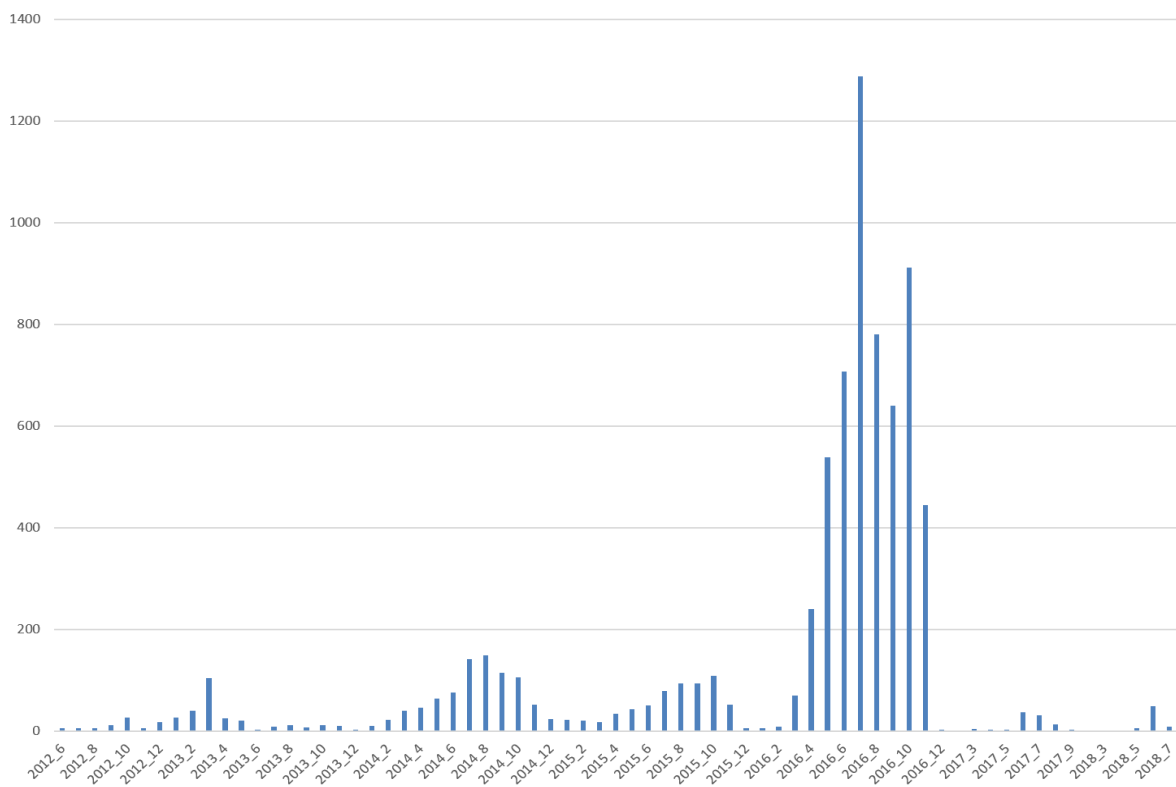
Table 2. Fixed and random effects included in the model, statistical coefficients and their standard deviations (SD) and 95% credible intervals.

	<b>Coefficient</b>	<b>SD</b>	<b>Credible 2.5%</b>	<b>Credible 97.5%</b>
<b>Cattle density (cattle per km<sup>2</sup>)</b>	10.002	0.01	10.001	10.002
<b>Land cover: croplands*</b>	20.666	0.16	15.074	28.499
<b>Land cover: grassland*</b>	17.020	0.20	11.573	25.143
<b>Land cover: permanent waterland*</b>	0.0042	12.51	0.0000	237993
<b>Land cover: shrubland*</b>	17.151	0.22	11.102	26.549
<b>Land cover: sparse*</b>	0.0655	1.01	0.0080	0.4294
<b>Annual mean temperature (°C)</b>	13.320	0.03	12.555	14.148
<b>Mean temperature (°C) diurnal range**</b>	12.762	0.06	11.239	14.496
<b>Temperature (°C) seasonality***</b>	0.9999	0.00	0.9980	10.019
<b>Mean temperature (°C) of wettest quarter</b>	0.9809	0.02	0.9491	10.139
<b>Annual precipitation (mm)</b>	10.001	0.00	0.9987	10.014
<b>Precipitation (mm) seasonality****</b>	0.9832	0.01	0.9659	10.013
<b>Spatial structured random effect</b>	482.026	2.57		
<b>Spatial non-structured random effect</b>	0.0105	0.006		

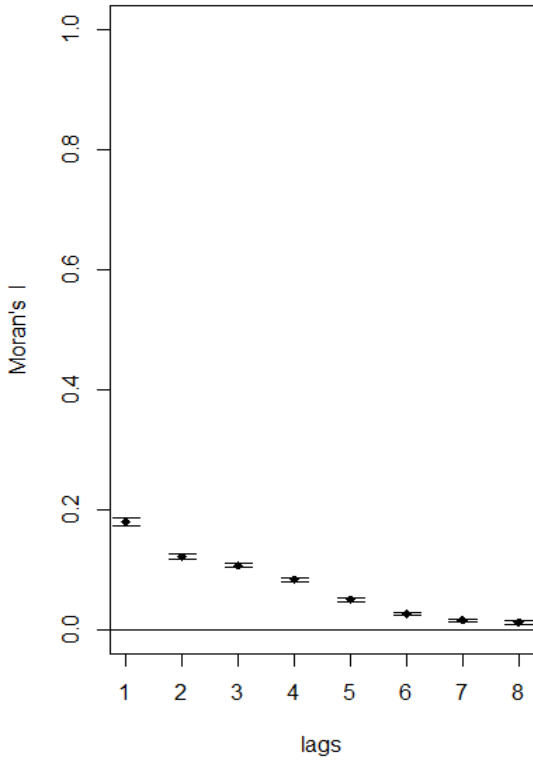
\*The reference category for land cover was forest. \*\*Mean temperature (°C) diurnal range: Mean of monthly (maximum temperature (°C) - minimum temperature (°C)). \*\*\*Temperature (°C) seasonality: standard deviation \*100. \*\*\*\*Precipitation (mm) seasonality: Coefficient of Variation.







Model without spatial random effects



Model with spatial random effects

